Corrected 11 April 2016; see full text.


7. N. Read, S. Sachdev, *Phys. Rev. B* **42**, 4568–4589 (1990).
8. G. Murthy, S. Sachdev, *Nucl. Phys. B* **344**, 557–595 (1990).
9. N. Read, S. Sachdev, *Phys. Rev. Lett.* **66**, 1773–1776 (1991).
10. O. I. Motrunich, A. Vishwanath, *Phys. Rev. B* **70**, 075104 (2004).
11. M. A. Metlitski, M. Hermele, T. Senthil, M. P. A. Fisher, *Phys. Rev. B* **78**, 214418 (2008).
12. E. Dyer, M. Mezei, S. S. Pufu, S. Sachdev, *J. High Energy Phys.* **2015**, 37 (2015).
13. T. Li, F. Becca, W. Hu, S. Sorella, *Phys. Rev. B* **86**, 075111 (2012).
14. S.-S. Gong, W. Zhu, D. N. Sheng, O. I. Motrunich, M. P. A. Fisher, *Phys. Rev. Lett.* **113**, 027201 (2014).
15. A. W. Sandvik, *Phys. Rev. Lett.* **98**, 227202 (2007).
16. R. G. Melko, R. K. Kaul, *Phys. Rev. Lett.* **100**, 017203 (2008).
17. F. J. Jiang, M. Nyfeler, S. Chandrasekharan, U.-J. Wiese, *J. Stat. Mech.* **2008**, P02009 (2008).
18. A. W. Sandvik, *Phys. Rev. Lett.* **104**, 177201 (2010).
19. R. K. Kaul, *Phys. Rev. B* **84**, 054407 (2011).
20. K. Harada *et al.*, *Phys. Rev. B* **88**, 220408 (2013).
21. K. Chen *et al.*, *Phys. Rev. Lett.* **110**, 185701 (2013).
22. M. S. Block, R. G. Melko, R. K. Kaul, *Phys. Rev. Lett.* **111**, 137202 (2013).
23. S. Pujari, F. Alet, K. Damle, *Phys. Rev. B* **91**, 104411 (2015).
24. A. Nahum, J. T. Chalker, P. Serna, M. Ortunõ, A. M. Somoza, *Phys. Rev. X* **5**, 041048 (2015).
25. G. J. Sreejith, S. Powell, *Phys. Rev. B* **89**, 014404 (2014).
26. A. B. Kuklov, M. Matsumoto, N. V. Prokof'ev, B. V. Svistunov, M. Troyer, *Phys. Rev. Lett.* **101**, 050405 (2008).
27. O. I. Motrunich, A. Vishwanath, http://arxiv.org/abs/0805.1494 (2008).
28. L. Bartosch, *Phys. Rev. B* **88**, 195140 (2013).
29. J. M. Luck, *Phys. Rev. B* **31**, 3069–3083 (1985).
30. A. W. Sandvik, V. N. Kotov, O. P. Sushkov, *Phys. Rev. Lett.* **106**, 207203 (2011).
31. F. Léonard, B. Delamotte, *Phys. Rev. Lett.* **115**, 200601 (2015).
32. Supplementary materials are available on *Science* Online.
33. Y. Tang, A. W. Sandvik, *Phys. Rev. Lett.* **107**, 157201 (2011).
34. A. Banerjee, K. Damle, *J. Stat. Mech.* **2010**, P08017 (2010).
35. Y. Tang, A. W. Sandvik, *Phys. Rev. Lett.* **110**, 217213 (2013).



**ACKNOWLEDGMENTS**

The research was supported by the National Natural Science Foundation of China, grant no. 11175018 (W.G.); the Fundamental Research Funds for the Central Universities (W.G.); U.S. NSF grant no. DMR-1410126 (A.W.S.); and the Simons Foundation (A.W.S.). H.S. and W.G. gratefully acknowledge support from the Condensed Matter Theory Visitors Program at Boston University, and A.W.S. is grateful to the Institute of Physics of the Chinese Academy of Sciences and to Beijing Normal University for their support. Some computations were carried out using Boston University's Shared Computing Cluster. We thank K. Damle for suggesting a definition of spinons that uses valence-bond strings. Computer code is available from the authors upon request.


**SUPPLEMENTARY MATERIALS**

www.sciencemag.org/content/352/6282/213/suppl/DC1
Supplementary Text
Figs. S1 to S10
References (*36*–*41*)

22 September 2015; accepted 1 March 2016
Published online 17 March 2016
10.1126/science.aad5007

BRAIN CONNECTIVITY

# Task-free MRI predicts individual differences in brain activity during task performance

**I. Tavor,[1,2] O. Parker Jones,[1] R. B. Mars,[1,3] S. M. Smith,[1] T. E. Behrens,[1,4] S. Jbabdi[1]***

**When asked to perform the same task, different individuals exhibit markedly different patterns of brain activity. This variability is often attributed to volatile factors, such as task strategy or compliance. We propose that individual differences in brain responses are, to a large degree, inherent to the brain and can be predicted from task-independent measurements collected at rest. Using a large set of task conditions, spanning several behavioral domains, we train a simple model that relates task-independent measurements to task activity and evaluate the model by predicting task activation maps for unseen subjects using magnetic resonance imaging. Our model can accurately predict individual differences in brain activity and highlights a coupling between brain connectivity and function that can be captured at the level of individual subjects.**

We all differ in how we perceive, think, and act. Our brains also differ in how they solve tasks. Understanding these individual differences in brain activity is an important goal in neuroscience, as it provides a route for linking brain and behavior.

Often, individual differences in brain activity induced by an experimental task are attributed to two possible factors. First, they may be accounted for by differences in gross brain morphology. The vast majority of brain-imaging studies rely on the spatial alignment of different brains (registration) to account for between-subject discrepancies in gross anatomy (*1*). Second, subjects may use different strategies or cognitive processes that involve different brain circuits. Psychologists design their tasks with great care to limit this source of variability. Nevertheless, individual variations are seen in all behavioral domains (*2*–*6*). These between-subject differences are often treated as "noise" in imaging studies and discarded through the process of averaging individual responses (*7*). Indeed, it is thought that such individual differences are mainly explained by volatile factors related to the behavior.

We investigated the possibility that individual differences in brain activation are inherent features of individuals and, to a large degree, independent of volatile factors. We explored the extent to which individual differences in task-evoked brain activity can be predicted by differences in the functional connectivity of the brain, acquired in a magnetic resonance imaging (MRI) scanner while the subjects are at rest and not performing any explicit task. We aimed to predict several task-evoked activity maps matching individual subject's maps in multiple behavioral domains based on a single task-free scan (i.e., unconstrained cognition during rest, with no explicit experimental task) of any given subject.

We designed a set of regression-based models that use task-independent features to predict individual task-evoked responses. Following the hypothesis that functional differentiation in the brain can be understood in terms of the underlying long-range brain connections and interactions (*8*, *9*), we used predictors based on functional connectivity at rest (*10*). Brain networks, extracted from resting-state data sets, qualitatively resemble task-evoked networks at the group level (*11*). We therefore hypothesized that, using functional connectivity at rest, we could predict individual variations in task responses. We also used predictors encoding individual brain morphology (gross structure) and microstructure to yield a total of 107 predictors [see Materials and Methods in supplementary materials (SM)]. All of our predictors were based on imaging subjects at rest and were independent of any given task. The model was trained to map between the predictors and task activations in a cohort of subjects for each task, and subsequently, the trained model was applied to out-of-sample (unseen) subjects to predict their task activations (a leave-one-out approach, see Materials and Methods in SM for details). Throughout, we focused on predicting task activations on the cortex, although the approach can easily be extended to incorporate subcortical gray matter.

Our data were a subset (98 subjects) of the Human Connectome Project (HCP) database (*12*). HCP data were chosen for their inclusion of resting-state measurements, diffusion-weighted MRI, and structural MRI, as well as task-evoked data spanning several behavioral domains. We could therefore use the same set of task-free data to test predictions of several different tasks. The HCP task data include seven behavioral domains, and each task set comprises several statistical maps pertaining to different aspects of each task

[1]Oxford Centre for Functional Magnetic Resonance Imaging of the Brain (FMRIB), Nuffield Department of Clinical Neurosciences, John Radcliffe Hospital, Oxford OX3 9DU, UK. [2]Department of Diagnostic Imaging, Sheba Medical Center, Tel Hashomer, 52621, Israel. [3]Donders Institute for Brain, Cognition and Behaviour, Radboud University Nijmegen, 6525 EZ Nijmegen, Netherlands. [4]Wellcome Trust Centre for Neuroimaging, University College London, London, WC1N 3BG, UK.
***Corresponding author. E-mail: saad@fmrib.ox.ac.uk**

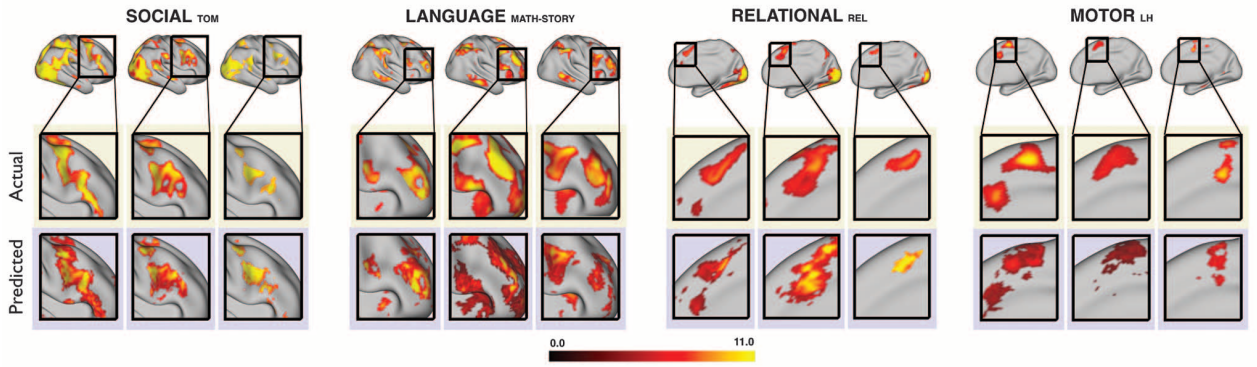


**Fig. 1. Predicting individual variations in task maps.** Figure shows actual and predicted thresholded task maps in three subjects and four different task contrasts. The model is able to capture striking variations between subjects in the shape, topology, and extent of their activation maps. Predictions and comparisons with actual maps for all behavioral domains and more subjects are shown in figs. S1 to S3 and movies S1 to S7.

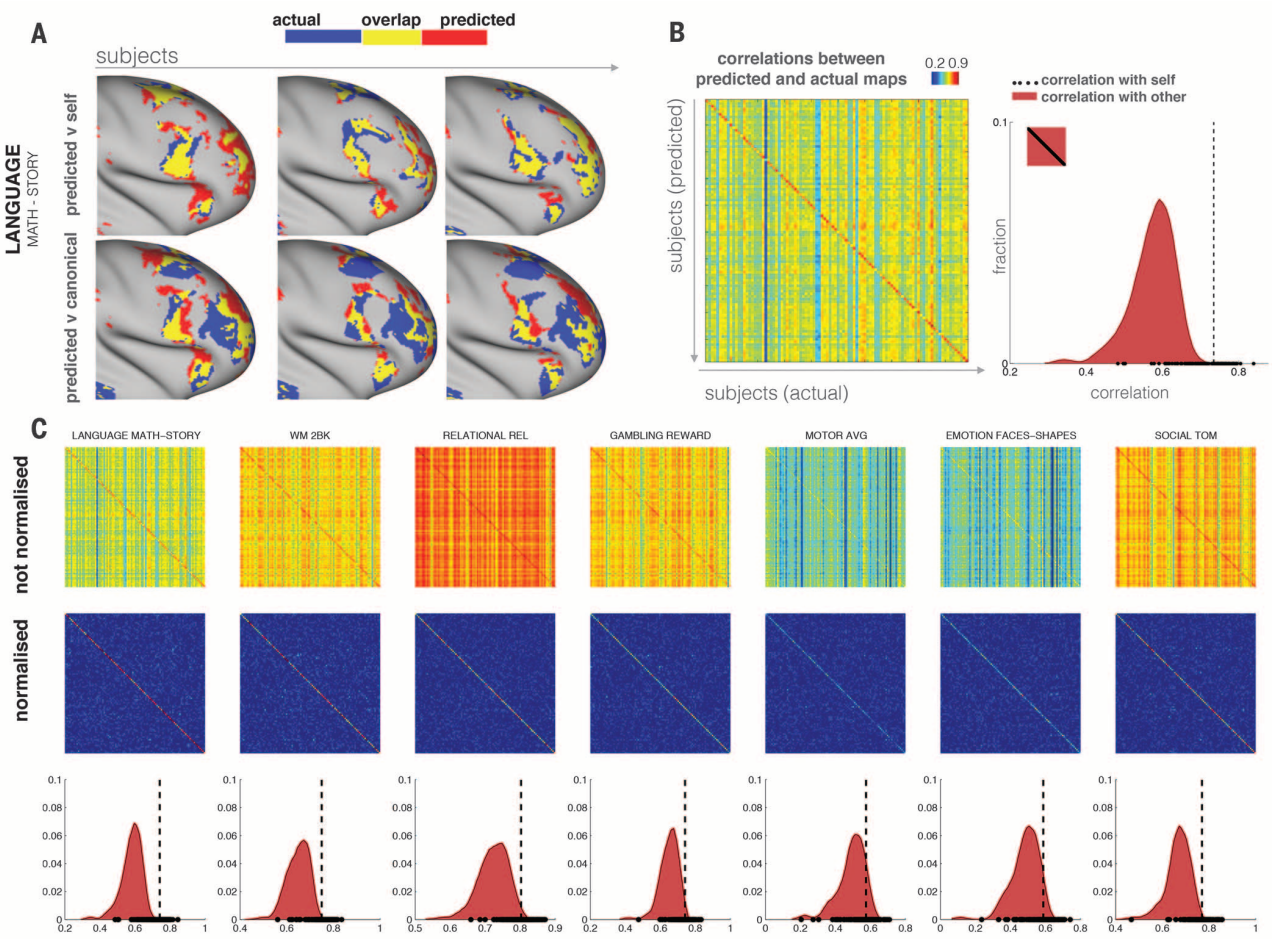


**Fig. 2. Specificity of the individual predictions.** A subject's predicted map is more similar to the subject's actual map than to the rest of the subjects. (**A**) Predicted maps (zoomed on the right frontal lobe) of the MATH-STORY contrast from the LANGUAGE task of three subjects are overlapped with their actual activation maps (top row). We also overlap the subjects' predictions with the activation map of the median subject (bottom row). Blue represents actual activation, red is the predicted activation, and yellow is the overlap. The maximum overlap is obtained when comparing a given subject's prediction with their own actual map. (**B**) Pearson correlation matrix between actual (columns) and predicted activations (rows). The correlation matrix is noticeably diagonal-dominant, which indicates that, on average, the model prediction for any given subject is more similar to the subject's own map than to other subjects' maps. This is also shown as a histogram plot, where the extradiagonal elements of the correlation matrix (subject X versus subject Y) are compared with the diagonal elements (subject X versus subject X). The vertical dashed line corresponds to the median of the correlation coefficients along the diagonal. (**C**) Correlation matrices and histograms for six additional behavioral domains. When we normalized the rows and columns of the correlation matrices (which removes the mean and accounts for higher variability in actual than in predicted maps), the diagonal-dominance is even more prominent. In all cases, a Kolmogorov-Smirnov test between the two distributions (self versus other) gives a highly significant difference ($P < 10^{-10}$).

Corrected 11 April 2016; see full text.

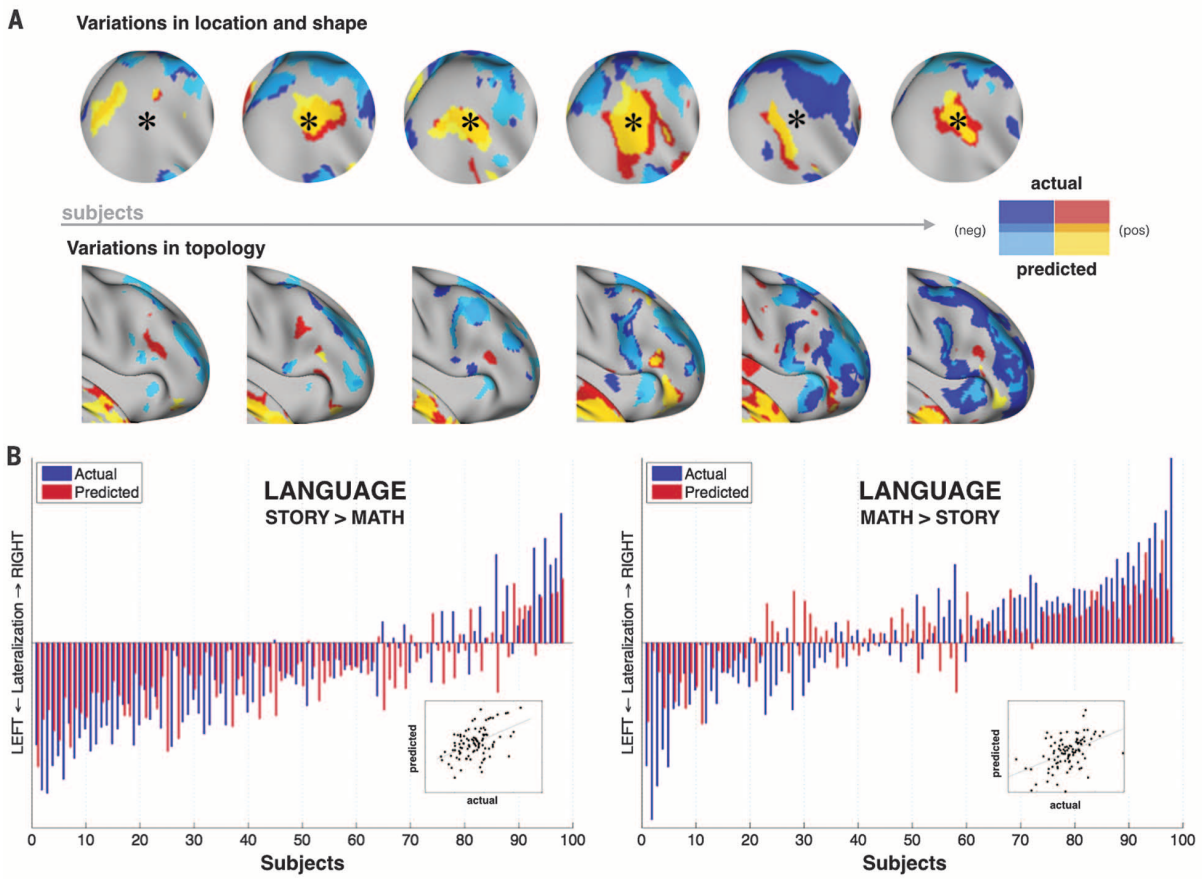


**Fig. 3. Capturing qualitative and quantitative interindividual differences.** (**A**) Variations in location, shape, and topology are predicted by the model (contrast: LANGUAGE MATH-STORY). (**B**) Peak *Z* scores were calculated for each hemisphere to examine how well the model can predict the amount of activation for each subject. A lateralization index (difference between right and left peak activation levels) is then calculated for each subject for both predicted and actual data and is shown as red and blue bars, respectively (LANGUAGE task). The model is able to predict individual subject's lateralization index for both contrasts, including the case where the majority of the subjects are left-lateralized. Statistical tests: MATH-STORY [correlation coefficient ($r$) = 0.47, $P < 10^{-5}$], STORY-MATH ($r$ = 0.48, $P < 10^{-6}$).

[all tasks and derived parametric maps are described in (*13*)]. A total of 47 independent task maps (*z* scores) were available for each subject (see Materials and Methods in SM).

We aimed to predict not how subjects activate on average in a given task but how they differ (from each other) in their activation patterns. This aspect of the model is illustrated (Fig. 1) in four different task conditions (maps thresholded as described in Materials and Methods). The model could predict qualitative differences between subjects, in terms of shape, position, size, and topography of activations. Similar individual variations predicted across more subjects and all behavioral domains used by the HCP are shown in figs. S1 to S3 and movies S1 to S7. The model could precisely predict individual task variations across all behavioral domains, on the basis of a single task-free data set. To get an impression of how similar our predictions are to the actual task maps, we overlapped the predictions for three subjects with their actual activation maps (Fig. 2A) for the contrast MATH-STORY of the LANGUAGE task. For comparison, we also overlapped the same subjects with the actual activation map of a canonical (median) subject. The maximum overlap was obtained when comparing a given subject's prediction with their actual map. This was despite our use of a leave-one-out approach: The predictive model for subject X had not seen the activation map of subject X during training, but it had seen the maps of all other subjects. Nevertheless, the prediction was more similar to the map it had not seen (subject X) than to the maps it had seen (all but subject X). The model did not learn what the activations for a given task looked like, but rather it learned how to map from the features (resting-state connectivity and morphology) to the task maps in individual subjects.

To quantitatively assess the performance of the model, we estimated the spatial correlation between the (unthresholded) predictions and actual maps for all pairs of subjects (Fig. 2, B and C). Each entry in the matrix is the Pearson correlation between the task map of one subject and the predicted map of another (off-diagonal) or the same (on-diagonal) subject. The correlation matrix is noticeably diagonal-dominant, which indicates that, on average, the model prediction for any given subject is more similar to the subject's own map than to other subjects' maps (see also the histograms shown in Fig. 2, B and C, comparing on-diagonal with off-diagonal entries). Normalizing rows and columns of the correlation matrix (which removes the overall mean correlation and accounts for the fact that the actual maps are more variable than the predicted maps) shows the diagonal-dominance even more clearly (see also figs. S4 to S6, in which we show the same results for all contrast maps). The diagonal-dominance is apparent for all tasks and contrast maps, with the exception of one contrast map (GAMBLING REWARD). The reason is that activations for this contrast are restricted to subcortical gray matter, whereas our model only makes predictions for the cortex. This result, i.e., the diagonal dominance of the spatial correlation matrix, is nontrivial considering that our leave-one-out procedure ensures that, whenever a model is applied to predict a given subject, it has never seen that subject's task map during training. Yet, the prediction matches that subject's task data better than the subjects that it has seen during training. The model's ability to generalize beyond the training subjects has important implications. It can predict activations in individuals for which there are no available task data (e.g., patients who cannot perform the task).

Corrected 11 April 2016; see full text.



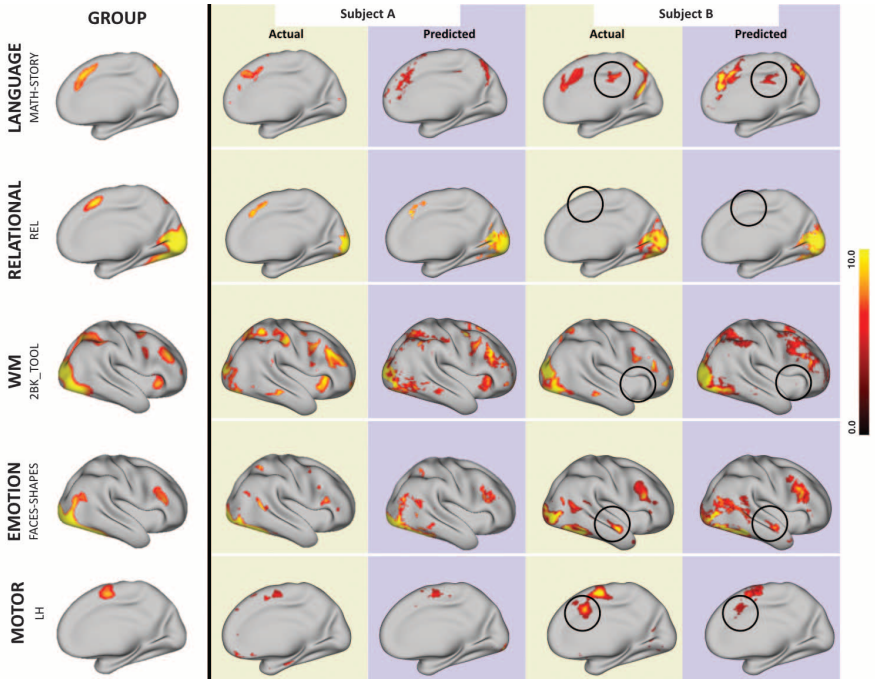


**Fig. 4. Predictions in atypical subjects.** The figure demonstrates the ability of our prediction model to detect intersubject variability when subjects differ from the group-averaged activation. In each row, the group activation for each behavioral domain is shown on the left, and the actual and predicted activations for two subjects are shown on the right. In each row, we show activations and predictions for one subject (A), whose activation is similar to the group activation, and another (B) who differs from it, as shown by the black circles. The model can capture the presence of clusters that are not active in the group (rows 1, 4, and 5), as well as the absence of clusters that are active in the group (rows 2 and 3). Note that subjects A and B are not the same pair of subjects across behavioral domains.

The model can precisely capture interindividual variability (table S3). There are different types of such variations. Functional brain areas in individual subjects can greatly vary in size, location, and shape (*14*). Primary visual cortex, for instance, can vary (across different subjects) by a factor of two or more in surface area (*15*). Such variability still allows one-to-one mapping of brain areas across subjects, provided that individual areas can be mapped in individual subjects. But another type of variation is topological variability, which for example means that different subjects may have different patterns of activity with no obvious one-to-one correspondence between subjects. Both types of variability (shape or size versus topological) can be captured by this model (Fig. 3A). Note that topological variability cannot be accounted for using spatial alignment between subjects, and thus, comparing or averaging subjects' activations when they have different topologies is an open problem. The fact that we can predict such variability from task-free data may enable new strategies for matching brain networks, as opposed to brain areas, across subjects.

Our model can also make predictions on the distribution of activity across different systems, such as in the case of hemispheric lateralization. Lateralization of function is seen commonly in the domain of language (*16*) but also in attentional processing (*17*). Our model can predict such differences across individuals in a language task, as shown in Fig. 3B. We estimated a lateralization index defined as the difference between right hemisphere and left hemisphere peak $Z$ (averaged over a 10-mm radius sphere around the predicted peak) from the predictions and the actual data. The model is able to precisely predict an individual subject's lateralization index. We also predicted two different contrasts from the same task (MATH-STORY and STORY-MATH), where the former tends to show an approximately equal distribution among left- and right-lateralized individuals, and the latter shows more left-lateralized subjects. The model can capture the lateralized language trend, even for the minority of right-lateralized subjects, despite the fact that, for the STORY-MATH contrast, it has been trained on subjects the majority of whom are left-lateralized.

The model could also predict atypical activation patterns. In Fig. 4, we show in five different behavioral domains examples of subjects that either do or do not conform to the pattern seen in the average subject. The model predicted activations in regions that were not activated on average. Conversely, the model correctly predicted the lack of activations in regions that were activated on average.

Overall, a simple set of models trained to learn a mapping between task-free and task-evoked maps could be used to predict individual differences in activation maps accurately across a wide range of behavioral domains. The predicted maps matched even large individual variations in the spatial layout of brain activity, including position, shape, size, and topology of functional activations (e.g., whether the activity is localized or spread out, or whether it consists of a single region or multiple subregions). The model could also predict individual differences in the amount of activation in a given task from a task-free data set.

The model mainly used resting-state connectivity in addition to a few structural features capturing local morphology and microstructure (see Materials and Methods in SM). On average across all tasks, all features participated in the predictions except for subcortical connectivity features (excluding the cerebellum—see figs. S7 and S8). Although the structural features were exploited by the model (fig. S7), removing them did not affect the performance of the model (fig. S9), and using a model purely based on structural features abolishes interindividual variability in the predictions (fig. S10). This suggests that resting-state connectivity alone is sufficient to predict individual variability in task maps, independently from variations of morphology as captured by our handful of structural features. It is, however, possible that additional anatomical variability may also be indirectly captured by the resting-state data.

Why can we predict task-evoked activity from resting-state data? A good match between resting-state networks and task networks at the group level has been shown before (*11*, *18*), where it has been argued that functional networks are continuously interacting with each other at rest, with the same functional hierarchy that is seen during action and cognition. Our model provides an explicit mapping from resting-state data to task maps that corroborates this assumption, but it is important to consider alternative explanations of our result. Intersubject alignment may be suboptimal when using anatomy alone. Our model is therefore possibly accounting for functional misalignment between subjects (*19*). However, the model not only tracks variation in the position and shape of functional areas but also captures variations in the topology of the brain networks activated in individual subjects and can predict activations of atypical subjects. Therefore, it is unlikely that the standard approach of aligning subjects while preserving the brain topology will be able to fix these types of misalignments. Our model can make quantitative predictions, in terms of the amount of activity that individual subjects display during a task. Such predictions are unlikely to arise from misalignment considerations. Resting-state data may provide a means for "calibration" of the blood oxygen–level–dependent (BOLD) signal (*20*). However, our predictors are based on measures of connectivity rather than raw BOLD signal strength per se [although signal-to-noise may still affect functional connectivity at rest (*21*)]. Determining what information in the resting-state signal is driving our predictions will be important for understanding its nature and potential. Because all the predictors that were used in this study are

Corrected 11 April 2016; see full text.

based on scans acquired at rest, our model is blind to different strategies that are chosen by the participants in performing a given task. We refer to these features as "inherent," but we acknowledge that these can be "structurally inherent" (related to brain organization and connectivity) or "functionally inherent" (related to the cognitive state of subjects during the resting-state scan).

The idea that brain connectivity can predict activation has previously been reported for different modalities (*22*, *23*), where diffusion MRI tractography was used (*24*) to measure connectivity. This study was limited to a number of visual contrasts. More recently, resting-state connectivity has been shown to be predictive of subjects' identity, in a way similar to a fingerprint (*25*). Rather than simply identifying subjects, our goal was to predict the entire layout of brain activity for each subject. Moreover, we also aim to predict such layout of activity in a number of different cognitive domains, from a single task-free scan, including in subjects that show patterns of activation that are different from the group average (perhaps most strikingly in right-lateralized subjects when the majority of training subjects are left-lateralized).

There are important practical implications of the proposed framework in basic research and translational neuroscience. It provides a method for inferring multiple individualized functional localizers based on a single resting-state scan. Such a tool could be used to investigate in detail the response profiles of localized brain regions without the need to acquire often time-consuming task localizers. Such a tool, if generalizable beyond the young, healthy population that makes up the HCP database, could be used to investigate functional regions in subjects who cannot perform tasks, such as infants or paralyzed patients.

## REFERENCES AND NOTES


1. M. Jenkinson, S. Smith, *Med. Image Anal.* **5**, 143–156 (2001).
2. J. Besle, R. M. Sánchez-Panchuelo, R. Bowtell, S. Francis, D. Schluppeck, *J. Neurophysiol.* **109**, 2293–2305 (2013).
3. F. McNab, T. Klingberg, *Nat. Neurosci.* **11**, 103–107 (2008).
4. I. Mukai *et al.*, *J. Neurosci.* **27**, 11401–11411 (2007).
5. S. M. Tom, C. R. Fox, C. Trepel, R. A. Poldrack, *Science* **315**, 515–518 (2007).
6. G. S. Wig *et al.*, *Proc. Natl. Acad. Sci. U.S.A.* **105**, 18555–18560 (2008).
7. R. Kanai, G. Rees, *Nat. Rev. Neurosci.* **12**, 231–242 (2011).
8. T. E. Behrens, H. Johansen-Berg, *Philos. Trans. R. Soc. Lond. B Biol. Sci.* **360**, 903–911 (2005).
9. R. E. Passingham, K. E. Stephan, R. Kötter, *Nat. Rev. Neurosci.* **3**, 606–616 (2002).
10. B. T. T. Yeo *et al.*, *J. Neurophysiol.* **106**, 1125–1165 (2011).
11. S. M. Smith *et al.*, *Proc. Natl. Acad. Sci. U.S.A.* **106**, 13040–13045 (2009).
12. D. C. Van Essen *et al.*, *Neuroimage* **80**, 62–79 (2013).
13. D. M. Barch *et al.*, *Neuroimage* **80**, 169–189 (2013).
14. B. Fischl *et al.*, *Cereb. Cortex* **18**, 1973–1980 (2008).
15. T. J. Andrews, S. D. Halpern, D. Purves, *J. Neurosci.* **17**, 2859–2868 (1997).
16. S. Knecht *et al.*, *Brain* **123**, 74–81 (2000).
17. M. Thiebaut de Schotten *et al.*, *Science* **309**, 2226–2228 (2005).
18. M. W. Cole, D. S. Bassett, J. D. Power, T. S. Braver, S. E. Petersen, *Neuron* **83**, 238–251 (2014).
19. E. C. Robinson *et al.*, *Neuroimage* **100**, 414–426 (2014).
20. N. K. Logothetis, B. A. Wandell, *Annu. Rev. Physiol.* **66**, 735–769 (2004).
21. K. J. Friston, *Brain Connect.* **1**, 13–36 (2011).
22. Z. M. Saygin *et al.*, *Nat. Neurosci.* **15**, 321–327 (2012).
23. D. E. Osher *et al.*, *Cereb. Cortex* **26**, 1668–1683 (2016).
24. P. J. Basser, S. Pajevic, C. Pierpaoli, J. Duda, A. Aldroubi, *Magn. Reson. Med.* **44**, 625–632 (2000).
25. E. S. Finn *et al.*, *Nat. Neurosci.* **18**, 1664–1671 (2015).


## ACKNOWLEDGMENTS

Data were provided by the Human Connectome Project, WU-Minn Consortium (Principal Investigators: D. Van Essen and K. Uğurbil; 1U54MH091657) funded by the 16 NIH Institutes and Centers that support the NIH Blueprint for Neuroscience Research; and by the McDonnell Center for Systems Neuroscience at Washington University in St. Louis. The data are available for download at www.humanconnectome.org. Data from the Q3 release (September 2013) were used in this paper. All code available upon request from the corresponding author. Funding was provided by the U.K. Medical Research Council (MR/L009013/1 to S.J.), U.K. Engineering and Physical Sciences Research Council (EP/L023067/1 to S.J. and T.E.B.), James S. McDonnell Foundation (JSMF220020372 to T.E.B.), the Wellcome Trust (WT104765MA to T.E.B. and 098369/Z/12/Z to S.M.S.), and the Netherlands Organization for Scientific Research (NWO) (452-13-015 to R.B.M.). Author contributions were as follows: S.J. and I.T. built the model and performed the analyses. S.J., I.T., R.B.M., O.P.J., S.M.S., and T.E.B. wrote the paper.

## SUPPLEMENTARY MATERIALS

www.sciencemag.org/content/352/6282/216/suppl/DC1
Materials and Methods
Figs. S1 to S23
Tables S1 to S3
Captions for Movies S1 to S7
References (*26*–*39*)
Movies S1 to S7

5 November 2015; accepted 29 February 2016
10.1126/science.aad8127

POLITICAL SCIENCE

# Durably reducing transphobia: A field experiment on door-to-door canvassing

**David Broockman[1]* and Joshua Kalla[2]**

**Existing research depicts intergroup prejudices as deeply ingrained, requiring intense intervention to lastingly reduce. Here, we show that a single approximately 10-minute conversation encouraging actively taking the perspective of others can markedly reduce prejudice for at least 3 months. We illustrate this potential with a door-to-door canvassing intervention in South Florida targeting antitransgender prejudice. Despite declines in homophobia, transphobia remains pervasive. For the intervention, 56 canvassers went door to door encouraging active perspective-taking with 501 voters at voters' doorsteps. A randomized trial found that these conversations substantially reduced transphobia, with decreases greater than Americans' average decrease in homophobia from 1998 to 2012. These effects persisted for 3 months, and both transgender and nontransgender canvassers were effective. The intervention also increased support for a nondiscrimination law, even after exposing voters to counterarguments.**

Intergroup prejudice, defined broadly as negative attitudes about an outgroup, is a root cause of numerous adverse social, political, and health outcomes (*1*–*3*). Influential theories depict intergroup prejudices as deeply ingrained during childhood and highly resistant to change thereafter (*4*–*6*). Consistent with these theories, empirical research has found that durably reducing prejudice is challenging. Mass media interventions and other brief stimuli usually fail to reduce prejudiced attitudes (*7*) or have only temporary effects (*8*); lasting change appears to require intense intervention over months (*9*, *10*). Rare are studies demonstrating prejudice-reduction interventions relatively brief in duration yet proven to have lasting effects (*4*).

Theories of active processing, however, suggest a method for even brief interventions to durably change attitudes. A recurring finding of laboratory studies is that brief messages can durably change individuals' attitudes when individuals engage in active, effortful, processing (known as "System 2" processing) of those messages (*11*). These studies, conducted on other topics, raise the possibility that brief interventions encouraging active consideration of counter-prejudicial thoughts could produce lasting changes in attitudes toward an outgroup. Perspective-taking, "imagining the world from another's vantage point," is one

[1]Graduate School of Business, Stanford University, Stanford, CA, USA. [2]Department of Political Science, University of California, Berkeley, CA, USA.
*Corresponding author. E-mail: dbroockman@stanford.edu

**Task-free MRI predicts individual differences in brain activity during task performance**
I. Tavor, O. Parker Jones, R. B. Mars, S. M. Smith, T. E. Behrens and S. Jbabdi (April 7, 2016)
*Science* **352** (6282), 216-220. [doi: 10.1126/science.aad8127]

Editor's Summary

**Every brain is different**

We all differ in how we perceive, think, and act. What drives individual differences in evoked brain activity? Tavor *et al*. applied computational models to functional magnetic resonance imaging (fMRI) data from the Human Connectome Project. Brain activity in the "resting" state when subjects were not performing any explicit task predicted differences in fMRI activation across a range of cognitive paradigms. This suggests that individual differences in many cognitive tasks are a stable trait marker. Resting-state functional connectivity thus already contains the repertoire that is then expressed during task-based fMRI.

*Science*, this issue p. 216



*Science* (print ISSN 0036-8075; online ISSN 1095-9203) is published weekly, except the last week in December, by the American Association for the Advancement of Science, 1200 New York Avenue NW, Washington, DC 20005. 